Efficient Analysis of Waveguide-to-Microstrip and Waveguide-to-Coplanar Line Transitions

Łukasz Gręda and Reinhold Pregla

FernUniversität, D-58084 Hagen, Germany

Abstract — **A general procedure using the Method of Lines for the analysis of waveguide-to-microstrip and waveguide-to-coplanar line transitions is described. Using two crossed two-dimensional discretization line systems instead of a full three-dimensional discretization allows to reduce the numerical effort. This concept is combined with the concept of impedance/admittance transformation. The described relations are also useful for other applications. The proposed algorithm is validated by comparison to measured and theoretical results.**

I. Introduction

Waveguide-to-microstrip and waveguide-to-coplanar line transitions are essential parts of microwave circuits. There are several types of such transitions, to the most-known belong: a ridged-waveguide taper, a finline taper and an E-plane probe. A new transition type with a rectangular patch instead of a strip probe, which was proposed by Machac *et al.* [1] has significantly broader bandwidth. This new transition type can occur in two versions: microstrip and coplanar line (Fig. 1).

The Method of Lines, which was previously successfully applied to the analysis of rectangular waveguide junctions using two one-dimensional cross line systems [2] and impedance/admittance transformation concept [3], is now extended to the analysis of waveguide-to-microstrip and waveguide-to-coplanar line transitions, for which normally three-dimensional discretizations are required. The use of two crossed two-dimensional line systems for modeling a central region instead of a full three-dimensional discretization allows to significantly reduce the numerical effort. Additionally, to reduce the total number of lines needed for modeling the central region, a nonequidistant discretization can be used.

This procedure will be demonstrated with the example of the waveguide-to-microstrip transition given in Fig. 1a. The procedure for the analysis of waveguide-to-coplanar line transition is analogous.

For the structures depicted in Fig. 1 there are two possibilities of analysis – with the subdivision on two- or three-ports junction. In case of the two-ports analysis, more lines are needed to model the central region, but there are less impedance/admitance transformations performed and lower programming effort is required. The choice of the used subdivision method depends on the distance between the port P2 (Fig. 1a) and the backshort. In case when this distance is small, the two-ports analysis is more efficient, otherwise it is worth to use the three-ports analysis.

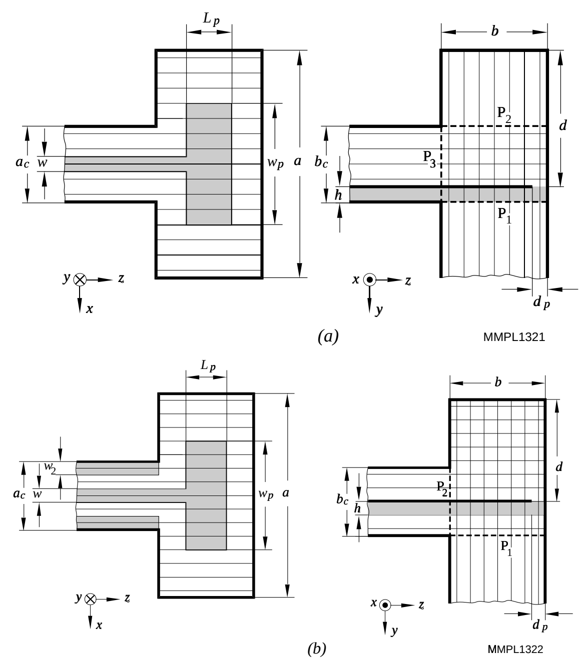

Fig. 1: Rectangular waveguide-to-microstrip (a) and waveguide-to-coplanar line (b) transitions with two possible discretization schemes.

The second type of the analysis (three-port) as a more general will be described as well. However the results presented here were obtained using the two-port analysis.

II. Theory

The discretization scheme for one of the discretization line systems (discretization lines in z direction) in the transition region is shown in Fig. 2. The discretization scheme for the other discretization line system (in y direction) is completely analogous. Details concerning discretization way were presented in [4]. The side walls of the connecting waveguides must be electric boundaries, therefore relations

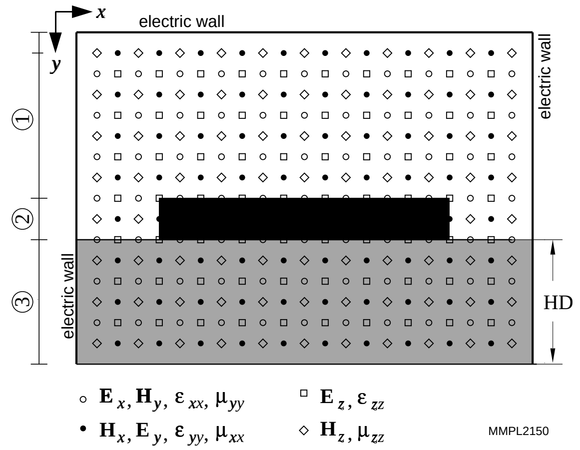

Fig. 2: Cross section of the transition region with discretization points.

of the field at the inner side of the ports P1, P2 and P3 can be described by short circuit matrix parameters:

$$\begin{bmatrix} \widehat{\overline{\mathbf{H}}}_{\mathrm{P1}} \\ -\widehat{\overline{\mathbf{H}}}_{\mathrm{P2}} \\ \widehat{\overline{\mathbf{H}}}_{\mathrm{P3}} \end{bmatrix} = \begin{bmatrix} \widehat{\overline{\boldsymbol{y}}}^{\mathrm{P1}}_{\mathrm{P1}} & \widehat{\overline{\boldsymbol{y}}}^{\mathrm{P2}}_{\mathrm{P1}} & \widehat{\overline{\boldsymbol{y}}}^{\mathrm{P3}}_{\mathrm{P1}} \\ \widehat{\overline{\boldsymbol{y}}}^{\mathrm{P1}}_{\mathrm{P2}} & \widehat{\overline{\boldsymbol{y}}}^{\mathrm{P2}}_{\mathrm{P2}} & \widehat{\overline{\boldsymbol{y}}}^{\mathrm{P3}}_{\mathrm{P2}} \\ \widehat{\overline{\boldsymbol{y}}}^{\mathrm{P1}}_{\mathrm{P3}} & \widehat{\overline{\boldsymbol{y}}}^{\mathrm{P2}}_{\mathrm{P3}} & \widehat{\overline{\boldsymbol{y}}}^{\mathrm{P3}}_{\mathrm{P3}} \end{bmatrix} \begin{bmatrix} \widehat{\overline{\mathbf{E}}}_{\mathrm{P1}} \\ \widehat{\overline{\mathbf{E}}}_{\mathrm{P2}} \\ \widehat{\overline{\mathbf{E}}}_{\mathrm{P3}} \end{bmatrix} \qquad (1)$$

The overlined values are determined in transformed domain and the hat ($\widehat{\ }$) stands for supervectors and supermatrices [4]. The vectors $\widehat{\overline{\mathbf{H}}}$ and $\widehat{\overline{\mathbf{E}}}$ contain tangential field components, e. g. for the port P3

$$\widehat{\overline{\mathbf{H}}}_{\mathrm{P3}} = \begin{bmatrix} -\widehat{\overline{\mathbf{H}}}^{\mathrm{P3}}_{\mathrm{x}} \\ \widehat{\overline{\mathbf{H}}}^{\mathrm{P3}}_{\mathrm{y}} \end{bmatrix} \qquad \widehat{\overline{\mathbf{E}}}_{\mathrm{P3}} = \begin{bmatrix} \widehat{\overline{\mathbf{E}}}^{\mathrm{P3}}_{\mathrm{y}} \\ \widehat{\overline{\mathbf{E}}}^{\mathrm{P3}}_{\mathrm{x}} \end{bmatrix} \qquad (2)$$

The admittance submatrices in (1) are obtained by short circuiting the ports. This procedure will be explained with three submatrices of (1) as examples.

A. Main diagonal submatrices

For the calculation of $\widehat{\overline{\boldsymbol{y}}}^{\mathrm{P1}}_{\mathrm{P1}}$ the ports P2 and P3 have to be short circuited. Then $\widehat{\overline{\boldsymbol{y}}}^{\mathrm{P1}}_{\mathrm{P1}}$ is the input admittance matrix. In the example of Fig. 1, the ports are connected via a concatenation of three different sections. In each of these sections, the tangential fields at the ends (A, B) of a section (Fig. 3) can be described by [4]

$$\begin{bmatrix} \widehat{\overline{\mathbf{H}}}_{\mathrm{A}} \\ -\widehat{\overline{\mathbf{H}}}_{\mathrm{B}} \end{bmatrix} = \begin{bmatrix} \widehat{\overline{\boldsymbol{y}}}_1 & \widehat{\overline{\boldsymbol{y}}}_2 \\ \widehat{\overline{\boldsymbol{y}}}_2 & \widehat{\overline{\boldsymbol{y}}}_1 \end{bmatrix} \begin{bmatrix} \widehat{\overline{\mathbf{E}}}_{\mathrm{A}} \\ \widehat{\overline{\mathbf{E}}}_{\mathrm{B}} \end{bmatrix} \qquad (3)$$

where
$$\widehat{\overline{\boldsymbol{y}}}_1 = \widehat{\overline{\mathbf{Y}}}_0 / \tanh(\widehat{\boldsymbol{\Gamma}}\overline{d}) \quad \widehat{\overline{\boldsymbol{y}}}_2 = -\widehat{\overline{\mathbf{Y}}}_0 / \sinh(\widehat{\boldsymbol{\Gamma}}\overline{d}) \qquad (4)$$

$\boldsymbol{\Gamma}$ is a propagation constants, $\widehat{\overline{\mathbf{Y}}}_0$ is a characteristic admittance matrix and $\overline{d} = k_0 d$ is a normalized distance between

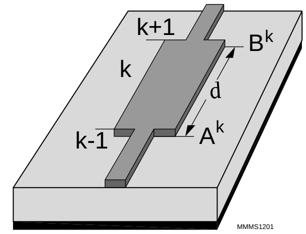

Fig. 3: Division of a structure into sections.

the planes. Hence, the admittance at the one end of an arbitrary section *k* can be obtain from the admittance at the second end of this section by

$$\widehat{\overline{\mathbf{Y}}}^k_{\mathrm{A}} = \widehat{\overline{\boldsymbol{y}}}^k_1 - \widehat{\overline{\boldsymbol{y}}}^k_2 \left(\widehat{\overline{\boldsymbol{y}}}^k_1 + \widehat{\overline{\mathbf{Y}}}^k_{\mathrm{B}} \right)^{-1} \widehat{\overline{\boldsymbol{y}}}^k_2 \qquad (5)$$

Transitions between sections can be calculated by

$$\widehat{\overline{\mathbf{Y}}}^{k-1}_{\mathrm{B}} = \widehat{\boldsymbol{T}}^{-1}_{\mathrm{H}_{k-1}} \boldsymbol{J}^{\mathrm{ct}}_{k-1} \left(\boldsymbol{J}^{\mathrm{c}}_k \widehat{\boldsymbol{T}}_{\mathrm{E}_k} \left(\widehat{\overline{\mathbf{Y}}}^k_{\mathrm{A}} \right)^{-1} \widehat{\boldsymbol{T}}^{-1}_{\mathrm{H}_k} \boldsymbol{J}^{\mathrm{ct}}_k \right)^{-1} \boldsymbol{J}^{\mathrm{c}}_{k-1} \widehat{\boldsymbol{T}}_{\mathrm{E}_{k-1}} \qquad (6)$$

where the eigenvector matrices $\boldsymbol{T}_{\mathrm{E,H}}$ [4] transform the field from the original to the transform domain, matrices $\boldsymbol{J}^{\mathrm{c}}$ reduce the field in the original domain to the common part on both sides of the transition. Due to the electric wall at the end, the input admittance matrix at the last subport k obtained from (3) becomes $\widehat{\overline{\boldsymbol{y}}}^k_1$. Transforming the admittance with (5) and (6) through all k sections (in the example shown in Fig. 1 $k = 3...1$) gives the input admittance matrix $\widehat{\overline{\boldsymbol{y}}}^{\mathrm{P1}}_{\mathrm{P1}}$.

The same procedure holds for the submatrices $\widehat{\overline{\boldsymbol{y}}}^{\mathrm{P2}}_{\mathrm{P2}}$ (in this case ports P1 and P3 must be short circuited) and $\widehat{\overline{\boldsymbol{y}}}^{\mathrm{P3}}_{\mathrm{P3}}$ (ports P1 and P2 are short circuited).

B. Off-diagonal submatrices

For the calculation of the matrices $\widehat{\overline{\boldsymbol{y}}}^{\mathrm{P2}}_{\mathrm{P1}}$ and $\widehat{\overline{\boldsymbol{y}}}^{\mathrm{P1}}_{\mathrm{P2}}$ the opposite transformation direction as for the main diagonal matrices must be used.

With the input admittance matrix, the before calculated admittances and (3), all the field vectors at the subports can be computed using the following matching equations:

$$\widehat{\overline{\mathbf{E}}}^k_{\mathrm{B}} = \left(\widehat{\overline{\boldsymbol{y}}}^k_2 \right)^{-1} \left(\widehat{\overline{\mathbf{Y}}}^k_{\mathrm{A}} - \widehat{\overline{\boldsymbol{y}}}^k_1 \right) \widehat{\overline{\mathbf{E}}}^k_{\mathrm{A}} \qquad (7)$$

$$-\widehat{\overline{\mathbf{H}}}^k_{\mathrm{B}} = \widehat{\overline{\boldsymbol{y}}}^k_2 + \widehat{\overline{\boldsymbol{y}}}^k_1 \left(\widehat{\overline{\boldsymbol{y}}}^k_2 \right)^{-1} \left(\widehat{\overline{\mathbf{Y}}}^k_{\mathrm{A}} - \widehat{\overline{\boldsymbol{y}}}^k_1 \right) \widehat{\overline{\mathbf{E}}}^k_{\mathrm{A}} \qquad (8)$$

$$\widehat{\overline{\mathbf{H}}}^k_{\mathrm{A}} = \widehat{\boldsymbol{T}}^{-1}_{\mathrm{H}_k} \boldsymbol{J}^{\mathrm{ct}}_k \widehat{\boldsymbol{T}}_{\mathrm{H}_{k-1}} \widehat{\overline{\mathbf{H}}}^{k-1}_{\mathrm{B}} \qquad (9)$$

$$\widehat{\overline{\mathbf{E}}}^k_{\mathrm{A}} = \left(\widehat{\overline{\mathbf{Y}}}^k_{\mathrm{A}} \right)^{-1} \widehat{\overline{\mathbf{H}}}^k_{\mathrm{A}} \qquad (10)$$

From the magnetic field obtained at the last subport $\widehat{\overline{\mathbf{H}}}_{\mathrm{B}}^{3}$, which is proportional to the input electric field $\widehat{\overline{\mathbf{E}}}_{\mathrm{A}}$, the matrices $\widehat{\overline{\boldsymbol{y}}}_{\mathrm{P1}}^{\mathrm{P2}}$ and $\widehat{\overline{\boldsymbol{y}}}_{\mathrm{P2}}^{\mathrm{P1}}$ can be obtained.

The other off-diagonal matrices represent coupling between ports.

Calculating these matrices will be explained with the submatrix $\widehat{\overline{\boldsymbol{y}}}_{\mathrm{P3}}^{\mathrm{P1}}$ as an example. Because of electric walls (ports P2 and P3 are short circuited), the tangential electric components produce only zero electric field. For this reason for the coupling from port P1 to port P3 only the tangential magnetic components are responsible

$$\widehat{\mathbf{H}}_{\mathrm{P3}} = \begin{bmatrix} \widehat{\mathbf{H}}_{\mathrm{x}}^{\mathrm{P3}} \\ \widehat{\mathbf{H}}_{\mathrm{z}}^{\mathrm{P3}} \end{bmatrix} \tag{11}$$

The calculations have to be done in parts, because the port P3 must be divided according to the sidewalls areas into k subports. The magnetic or electric field in a plane at an arbitrary position z between two subports A^k $(z=0)$ and B^k $z=d_k$ of a section k can be computed from the fields at the subports A^k and B^k using the following formula

$$\widehat{\overline{\mathbf{F}}}\left(z_i^k\right) = \boldsymbol{\Lambda}_{\mathrm{A}^k}^{d}\widehat{\overline{\mathbf{F}}}_{\mathrm{A}}^{k} + \boldsymbol{\Lambda}_{\mathrm{B}^k}^{d}\widehat{\overline{\mathbf{F}}}_{\mathrm{B}}^{k} \tag{12}$$

$\widehat{\overline{\mathbf{F}}}$ is the vector of the transversal electric or magnetic components. Both parts $\widehat{\overline{\mathbf{F}}}_{\mathrm{A}}^{k}$ and $\widehat{\overline{\mathbf{F}}}_{\mathrm{B}}^{k}$ are caused by fields at the port P1. The diagonal matrices $\boldsymbol{\Lambda}_{\mathrm{A}^k}^{d}$ and $\boldsymbol{\Lambda}_{\mathrm{B}^k}^{d}$ are given by

$$\boldsymbol{\Lambda}_{\mathrm{A}^k}^{d} = \frac{\sinh\left(\boldsymbol{\Gamma}_z^k \overline{z}_{-}\right)}{\sinh\left(\boldsymbol{\Gamma}_z \overline{d}_{\mathrm{AB}^k}\right)} \quad \boldsymbol{\Lambda}_{\mathrm{B}^k}^{d} = \frac{\sinh\left(\boldsymbol{\Gamma}_z^k \overline{z}\right)}{\sinh\left(\boldsymbol{\Gamma}_z \overline{d}_{\mathrm{AB}^k}\right)} \tag{13}$$

with $\overline{z}_{-} = \overline{d}_k - \overline{z}$ and $\overline{d}_k = k_0 d_k$. d_k is the distance between the ports A^k and B^k, $\boldsymbol{\Gamma}_z^k$ is a propagation constant.

The field component $\mathbf{H}_{\mathrm{x}}^{\mathrm{P3}}$ at the port P3 can be obtained by

$$\mathbf{H}_{\mathrm{x}}^{\mathrm{P3}}\left(z^k\right) = \boldsymbol{T}_{\mathrm{H_x}}^{\mathrm{P3}}\left(\boldsymbol{\Lambda}_{\mathrm{A}^k}^{d}\widehat{\overline{\mathbf{H}}}_{\mathrm{A}^k} + \boldsymbol{\Lambda}_{\mathrm{B}^k}^{d}\widehat{\overline{\mathbf{H}}}_{\mathrm{B}^k}\right) \tag{14}$$

where [5]

$$\boldsymbol{T}_{\mathrm{H_x}}^{\mathrm{P3}} = \frac{1}{8}\left(9\boldsymbol{T}_{\mathrm{H_{xN}}} - \boldsymbol{T}_{\mathrm{H_{xN_-}}}\right) \tag{15}$$

are the values of the field on the subports extrapolated from the values of the last and last but one rows of $\widehat{\boldsymbol{T}}_{\mathrm{Hx}}^{\mathrm{P3}}$. Discretizing the field component (14) at the discretization points z^k of the port P3 and collecting fields of all subports $\mathrm{P3^k}$, yields

$$\widehat{\mathbf{H}}_{\mathrm{x}}^{\mathrm{P3}} = \begin{bmatrix} \boldsymbol{T}_{\mathrm{H_x}}^{\mathrm{P3}}\boldsymbol{\Lambda}_{\mathrm{A}^1}^{d}\widehat{\overline{\mathbf{Y}}}_{\mathrm{AA}^1} + \boldsymbol{T}_{\mathrm{H_x}}^{\mathrm{P3}}\boldsymbol{\Lambda}_{\mathrm{B}^1}^{d}\widehat{\overline{\mathbf{Y}}}_{\mathrm{AB}^1} \\ \vdots \\ \boldsymbol{T}_{\mathrm{H_x}}^{\mathrm{P3}}\boldsymbol{\Lambda}_{\mathrm{A}^k}^{d}\widehat{\overline{\mathbf{Y}}}_{\mathrm{AA}^k} + \boldsymbol{T}_{\mathrm{H_x}}^{\mathrm{P3}}\boldsymbol{\Lambda}_{\mathrm{B}^k}^{d}\widehat{\overline{\mathbf{Y}}}_{\mathrm{AB}^k} \end{bmatrix} \overline{\mathbf{E}}_{\mathrm{P1}} = \widehat{\mathbf{Y}}_{\mathrm{xP3}}^{\mathrm{P1}}\widehat{\overline{\mathbf{E}}}_{\mathrm{P1}} \tag{16}$$

where

$$\widehat{\overline{\mathbf{H}}}_{\mathrm{A}^k} = \widehat{\overline{\mathbf{Y}}}_{\mathrm{AA}^k}\widehat{\overline{\mathbf{E}}}_{\mathrm{A}} \qquad \widehat{\overline{\mathbf{H}}}_{\mathrm{B}^k} = \widehat{\overline{\mathbf{Y}}}_{\mathrm{AB}^k}\widehat{\overline{\mathbf{E}}}_{\mathrm{A}} \tag{17}$$

The field vectors $\widehat{\overline{\mathbf{H}}}_{\mathrm{A}^k}$ and $\widehat{\overline{\mathbf{H}}}_{\mathrm{A}^k}$ caused by $\widehat{\overline{\mathbf{E}}}_{\mathrm{A}}$ were already calculated using (7)-(10). Eq. (16) is the upper part of the vector of (11).

The tangential magnetic field component $\mathbf{H}_{\mathrm{z}}^{\mathrm{P3}}$ can be obtain from

$$\mathbf{H}_{\mathrm{zn}}\left(z^k\right) = j\left[\widehat{\boldsymbol{D}}_{\overline{x}}^{\bullet} \;\; -\widehat{\boldsymbol{D}}_{\overline{y}}^{\circ}\right]\boldsymbol{T}_{\mathrm{E}}\widehat{\overline{\mathbf{E}}}\left(z^k\right) \tag{18}$$

where $\widehat{\boldsymbol{D}}_{\overline{x}}^{\bullet}$, $\widehat{\boldsymbol{D}}_{\overline{y}}^{\circ}$ are central differences in one row or one column.

To obtain the values $\mathbf{H}_{\mathrm{z}}^{\mathrm{P3}}$ at the port P3, similar procedure as for $\mathbf{H}_{\mathrm{x}}^{\mathrm{P3}}$ is required. The last two rows needed for extrapolation process can be obtained from

$$\mathbf{H}_{\mathrm{z}}\left(z^k\right) = j\left[\widehat{\boldsymbol{D}}_{\overline{x}}^{\bullet}\boldsymbol{T}_{\mathrm{E_{yn}}} \;\; -\widehat{\boldsymbol{D}}_{yn}^{\circ}\boldsymbol{T}_{\mathrm{E_{xn,n-1}}}\right]\widehat{\overline{\mathbf{E}}}\left(z^k\right) \tag{19}$$

where $\boldsymbol{T}_{\mathrm{E_y}}$, $\boldsymbol{T}_{\mathrm{E_x}}$ are parts of $\boldsymbol{T}_{\mathrm{E}}$ which correspond to the kind of the field components, and these two parts are further partitioned according to the *n* rows of the discretization points (see Fig. 2). $\widehat{\boldsymbol{D}}_{yn}^{\circ}\boldsymbol{T}_{\mathrm{E_{xn,n-1}}}$ is the difference of $\boldsymbol{T}_{\mathrm{E_{xn}}}$ and $\boldsymbol{T}_{\mathrm{E_{xn-1}}}$.

Discretizing the field component $\mathbf{H}_{\mathrm{z}}^{\mathrm{P3}}$ at the discretization points z^k of the port P3 and collecting the fields of all subports $\mathrm{P3}^k$, yields

$$\widehat{\mathbf{H}}_{\mathrm{z}}^{\mathrm{P3}} = \begin{bmatrix} \boldsymbol{T}_{\mathrm{H_z}}^{\mathrm{P3}}\boldsymbol{\Lambda}_{\mathrm{A}^1}^{d}\widehat{\overline{\mathbf{V}}}_{\mathrm{AA}^1} + \boldsymbol{T}_{\mathrm{H_z}}^{\mathrm{P3}}\boldsymbol{\Lambda}_{\mathrm{B}^1}^{d}\widehat{\overline{\mathbf{V}}}_{\mathrm{AB}^1} \\ \vdots \\ \boldsymbol{T}_{\mathrm{H_z}}^{\mathrm{P3}}\boldsymbol{\Lambda}_{\mathrm{A}^k}^{d}\widehat{\overline{\mathbf{V}}}_{\mathrm{AA}^k} + \boldsymbol{T}_{\mathrm{H_z}}^{\mathrm{P3}}\boldsymbol{\Lambda}_{\mathrm{B}^k}^{d}\widehat{\overline{\mathbf{V}}}_{\mathrm{AB}^k} \end{bmatrix} \overline{\mathbf{E}}_{\mathrm{P1}} = \widehat{\mathbf{Y}}_{\mathrm{zP3}}^{\mathrm{P1}}\widehat{\overline{\mathbf{E}}}_{\mathrm{P1}} \tag{20}$$

where

$$\widehat{\overline{\mathbf{E}}}_{\mathrm{A}^k} = \widehat{\overline{\mathbf{V}}}_{\mathrm{AA}^k}\widehat{\overline{\mathbf{E}}}_{\mathrm{A}} \qquad \widehat{\overline{\mathbf{E}}}_{\mathrm{B}^k} = \widehat{\overline{\mathbf{V}}}_{\mathrm{AB}^k}\widehat{\overline{\mathbf{E}}}_{\mathrm{A}} \tag{21}$$

The field vectors $\widehat{\overline{\mathbf{E}}}_{\mathrm{A}^k}$ and $\widehat{\overline{\mathbf{E}}}_{\mathrm{A}^k}$ which are proportional to $\widehat{\overline{\mathbf{E}}}_{\mathrm{A}}$ were determined earlier in this subsection. Eq. (20) is the lower part of the vector of (11).

The submatrix $\widehat{\boldsymbol{y}}_{\mathrm{P3}}^{\mathrm{P1}}$ can be written as follows

$$\widehat{\boldsymbol{y}}_{\mathrm{P3}}^{\mathrm{P1}} = \begin{bmatrix} \widehat{\boldsymbol{y}}_{\mathrm{xP3}}^{\mathrm{P1}} \\ \widehat{\boldsymbol{y}}_{\mathrm{zP3}}^{\mathrm{P1}} \end{bmatrix} \tag{22}$$

Since this matrix is in the original domain, it must be transformed using the transformation matrix $\widehat{\boldsymbol{T}}_{\mathrm{H}}^{P3}$

$$\widehat{\overline{\boldsymbol{y}}}_{\mathrm{P3}}^{\mathrm{P1}} = \left(\widehat{\boldsymbol{T}}_{\mathrm{H}}^{\mathrm{P3}}\right)^{-1}\widehat{\boldsymbol{y}}_{\mathrm{P3}}^{\mathrm{P1}} \tag{23}$$

It should be mentioned, that before multiplying, the components of $\widehat{\boldsymbol{y}}_{\mathrm{P3}}^{\mathrm{P1}}$ must be ordered in the same way as the components in the transformation matrix.

In an analogous way the remaining submatrices can be determined. Knowing all submatrices of (1), the input admittance matrix can be calculated. The admittance matrices at the inner side of the ports can be defined by

$$\widehat{\widehat{\mathbf{H}}}_{\mathrm{P1}} = \widehat{\widehat{\mathbf{Y}}}_{\mathrm{P1}} \widehat{\widehat{\mathbf{E}}}_{\mathrm{P1}} \quad -\widehat{\widehat{\mathbf{H}}}_{\mathrm{P2}} = \widehat{\widehat{\mathbf{Y}}}_{\mathrm{P2}} \widehat{\widehat{\mathbf{E}}}_{\mathrm{P2}} \quad \widehat{\widehat{\mathbf{H}}}_{\mathrm{P3}} = \widehat{\widehat{\mathbf{Y}}}_{\mathrm{P3}} \widehat{\widehat{\mathbf{E}}}_{\mathrm{P3}} \tag{24}$$

Introducing (24) into (1) and combining the ports admittance matrices, leads (for the port P3) to

$$\widehat{\widehat{\mathbf{Y}}}_{\mathrm{P3}} = \widehat{\overline{\boldsymbol{y}}}^{\mathrm{P3}}_{\mathrm{P3}} + \widehat{\overline{\mathbf{Y}}}^{\mathrm{P1P2}}_{\mathrm{P3}} \left(\widehat{\overline{\mathbf{Y}}}^{\mathrm{P1P2}}_{\mathrm{P1P2}} \right)^{-1} \widehat{\overline{\mathbf{Y}}}^{\mathrm{P3}}_{\mathrm{P1P2}} \tag{25}$$

where

$$\widehat{\overline{\mathbf{Y}}}^{\mathrm{P1P2}}_{\mathrm{P1P2}} = \begin{bmatrix} \widehat{\overline{\boldsymbol{y}}}^{\mathrm{P1}}_{\mathrm{P1}} - \widehat{\widehat{\mathbf{Y}}}_{\mathrm{P1}} & \widehat{\overline{\boldsymbol{y}}}^{\mathrm{P2}}_{\mathrm{P1}} \\ \widehat{\overline{\boldsymbol{y}}}^{\mathrm{P1}}_{\mathrm{P2}} & \widehat{\overline{\boldsymbol{y}}}^{\mathrm{P2}}_{\mathrm{P2}} - \widehat{\widehat{\mathbf{Y}}}_{\mathrm{P2}} \end{bmatrix} \tag{26}$$

$$\widehat{\overline{\mathbf{Y}}}^{\mathrm{P3}}_{\mathrm{P1P2}} = \begin{bmatrix} \widehat{\overline{\boldsymbol{y}}}^{\mathrm{P3}}_{\mathrm{P1}} & \widehat{\overline{\boldsymbol{y}}}^{\mathrm{P3}}_{\mathrm{P2}} \end{bmatrix}^{t} \quad \widehat{\overline{\mathbf{Y}}}^{\mathrm{P1P2}}_{\mathrm{P3}} = \begin{bmatrix} \widehat{\overline{\boldsymbol{y}}}^{\mathrm{P1}}_{\mathrm{P3}} & \widehat{\overline{\boldsymbol{y}}}^{\mathrm{P2}}_{\mathrm{P3}} \end{bmatrix} \tag{27}$$

With the input admittance matrix and the source mode, the fields at all ports can be obtained, and from these fields, the scattering parameters can be computed.

III. Results

To validate the proposed method of analysis, the reflection coefficient of the structure showed in the Fig. 1a have been calculated and compared with experimental [1] and theoretical result using FDTD + modal BC [6].

The waveguide type WR90 was examined and the substrate with permittivity ϵ_r = 2.35 was used.

The reflection coefficient obtained with the method described in this paper is showed in the Fig. 1. This result is with good agreement with experimental and theoretical results. The slightly lower reflection coefficient as for the measured result is obtained, because an ideal metal and substrate were assumed.

IV. Conclusion

A new general method for the efficient analysis of waveguide-to-microstrip and waveguide-to-coplanar line transitions is proposed and described. The use of two-dimensional discretization with crossed lines in the central region instead of three-dimensional discretization allows to calculate such structures very efficient. The admittance transformation concept used in this method is numerically stable and gives correct results even for long sections. An extension of this method to other types of waveguide transitions is very easy.

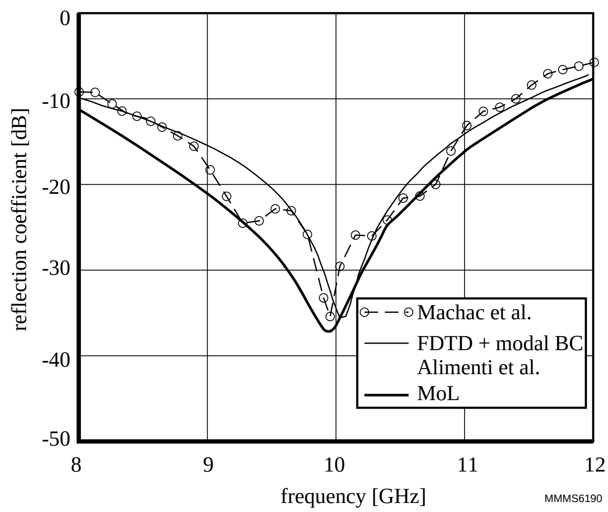

Fig. 4: Magnitude of the reflection coefficient of the waveguide-to-microstrip transition. The dimensions of the structure (description in Fig. 1a) are: a = 22.86mm, b = 10.16mm, h = 0.794mm, w = 2.3mm, L_p = 6mm, w_p = 12 mm, d_p = 3.16mm, d = 5.3mm, a_c = 8.0mm, b_c = 5.0mm

References

[1] J. Machac and W. Menzel, “On the design of waveguide-to-microstrip and waveguide-to-coplanar line transitions”, *23rd European Microwave Conf.*, Madrid, Spain, Sept. 1993, pp. 615–616.

[2] W. Pascher and R. Pregla , “Analysis of Rectangular Waveguide Junctions by the Method of Lines”, *IEEE Trans. Microwave Theory and Tech.*, vol. 43, no. 12, pp. 2649–2653, Dec. 1995.

[3] R. Pregla, “MoL-Analysis of Rectangular Waveguide Junctions by an Impedance/Admittance Transfer Concept and Crossed Discretisation Line”, *Internat. Journal of Electronics and Communications AEÜ*, vol. 53, no. 2, pp. 83–91, 1999.

[4] R. Pregla, “Efficient and Accurate Modeling of Planar Microwave Structures with Anisotropic Layers by the Method of Lines (MoL)”, *Internat. Symposium on Recent Advances in Microwave Technology*, Malaga, Spain, Dec. 1999, pp. 699–703.

[5] R. Pregla, “The Analysis of General Axially Symetric Antennas with a Coaxial Feed Line by the Method of Lines”, *IEEE Trans.on Antennas and Propagation*, vol. 46, no. 10, pp. 1433–1443, Oct. 1998.

[6] F. Alimenti et al., “A Revised Formulation of Modal Absorbing and Matched Modal Source Boundary Conditions for the Efficient FDTD Analysis of Waveguide Structures”, *IEEE Trans. Microwave Theory and Tech.*, vol. 48, no. 1, pp. 50–59, Jan. 2000.